Optics Letters

LITES: rotational Raman spectra of air molecules measured by high-resolution-spectroscopy lidar

Boyan Tatarov* and Detlef Müller

Department of Physics, Astronomy and Mathematics, University of Hertfordshire, College Lane, Hatfield, UK
**Corresponding author: b.tatarov@herts.ac.uk*

Received 19 January 2021; revised 4 March 2021; accepted 25 March 2021; posted 26 March 2021 (Doc. ID 420070); published 11 October 2021

We present the first, to the best of our knowledge, measurements from a new lidar facility that was designed and built at the University of Hertforshire since 2012. LITES (Lidar Innovations for Technologies and Environmental Sciences) allows testing, developing, and measuring of a multitude of climate-change relevant parameters of atmospheric particulate pollution and photochemically reactive trace gases. The core of LITES consists of a lidar spectroscopy instrument. In this first contribution, for example, we present the design and specifications of this instrument, its performance, and potential applications. First, we show examples of the measurements of range-resolved pure rotational Raman spectra and rotational-vibrational Raman spectra of air molecules with a spectral resolution better than 5 cm^{-1}. We also present day-time temperature profiles obtained from pure rotational spectroscopic lidar signals. In future work, we aim to explore the potential of our multi-channel high-resolution spectrometric lidar to obtain vertically resolved chemical characterization of aerosols and trace gases.

https://doi.org/10.1364/OL.420070

Lidar is the method of choice for measuring atmospheric state parameters, photochemically reactive trace gases and particulate pollution on a vertically highly resolved scale [1,2]. The combination of various lidar techniques (nitrogen Raman [3] and high spectral resolution lidar [4]) with mathematical inversion algorithms today allows for temporally and vertically resolved observations of aerosol optical and microphysical properties on a routine basis [5,6]. This approach of using Raman lidar and an inversion algorithm for particle characterization is limited to nighttime observations because of the weak intensity of Raman signals in the visible wavelength range (VIS). To the best of our knowledge, only NASA Langley's airborne multiwavelength high spectral resolution lidar (HSRL-2) allows for carrying out this type of combined optical and microphysical particle characterization also under daytime conditions [6,7]. Lidar and passive remote sensing instruments currently cannot provide us with vertically resolved information regarding the chemical composition of aerosols under ambient conditions.

Pure rotational Raman (PRR) lidar techniques and data analysis have been developed in the past 40 years and commonly used for atmospheric temperature measurements [8–10]. PRR lidar also allows for independent measurements of profiles of aerosol extinction and backscatter coefficients [11]. Both approaches, i.e., temperature and aerosol measurements, are usually based on the use of two or three separate channels for detecting different parts of the PRR spectra (PRRS) of air molecules. These traditional systems use combinations of interference filters, single or double monochromators, or Fabry–Perot etalons. Although these lidar show good performance with regard to temperature and aerosol profiling, they have several significant disadvantages: (1) these lidars are not able to provide simultaneous measurements of the entire PRRS; (2) the hardware is fixed in the sense that only one pumping wavelength can be used; (3) worldwide, only a few systems with very specific design are capable of carrying out day-time observations.

The long-term goal of our work is to explore the potential of using a multi-channel high-resolution spectrometric lidar for the vertically resolved chemical characterization of aerosols and gases based on the measurements of range-resolved Raman spectra. For that purpose, we have been developing a new remote sensing facility called Lidar Innovations for Technologies and Environmental Sciences (LITES). The facility combines a unique lidar spectroscopy instrument (LiSsI) with *in situ* instruments such as Raman and fluorescence microscopes, and gas and aerosol chambers.

In this Letter, we present the setup of LiSsI and show the results of the first measurements. The design of this lidar allows for the profiling of trace gases, chemical components in particles, and bio-aerosols in atmospheric aerosol pollution in the troposphere. The long-term goal can be achieved by combining different linear and nonlinear spectroscopy techniques, i.e., photoluminescence, fluorescence, Raman, and coherent anti-Stokes Raman spectroscopy in a single measurement platform.

The specifications of the system are listed in Table 1. The main components of the lidar include

- an ultra-high-energy seeded Nd:YAG laser (Continuum Powerlite Furie LD) with a second-harmonic generator and a third-harmonic generator. The system emits laser light with

Table 1. Technical Specifications of the Lidar System

Continuum Powerlite Furie LD	
Laser type	Nd:YAG, injection seeded
Pulse energy	8000 mJ at 1064 nm
	5000 mJ at 532 nm
	2500 mJ at 355 nm
Beam divergence	0.5 mrad
Repetition rate	10 Hz
Linewidth	$<0.003\ cm^{-1}$
Pulse duration	<15 ns
Horizon Optical Parametric Oscillator	
Pump wavelength	355 nm
Wavelengths	from 192 to 2750 nm
Resolution/scan step	0.01 nm
Pulse energy	120 mJ at 400 nm
	60 mJ at 600 nm
	25 mJ at 300 nm
	5 mJ at 200 nm
Beam divergence	<2 mrad (both axes)
Repetition rate	10 Hz
HORIBA 1250M Research Spectrometer	
Focal length	1.25 m, F/9
Spectral range	0–1500 nm at 1200 g/mm
Grating size	110 mm × 110 mm
Dispersion @500 nm	0.65 nm/mm
Accuracy/repeatability	±0.15 nm/ ± 0.005 nm
Gratings and blaze	max resolutions at 313.183 nm
2400 gr/mm at 250 nm	0.003 nm
1800 gr/mm at 400 nm	0.004 nm
1200 gr/mm at 330 nm	0.006 nm
600 gr/mm at 500 nm	0.012 nm
Detection Units	
Mie and Rayleigh Scattering	355 nm, PMT HV-R9880U-20 532 nm, PMT HV-R9880U-20 1064 nm, APD InGaAs50, Si-photodiode
Spectroscopic 1 Licel SP32-20	Hamamatsu H7260-20, 0.8 mm × 7 mm × 32 anodes spectral response 300–920 nm
Spectroscopic 2 Princeton Instruments PI-MAX4 ICCD camera	Number of pixels 1024 × 1024 Pixels size 16 × 16 μm Gen III filmless intensifier Sensitive range 290–710 nm
Spectroscopic 3 ANDOR iXon 3 EMCCD camera	Number of pixels 512 × 512 Pixels size 12.8 × 12.8 μm Sensitive range 300–710 nm
Schmidt–Cassegrain Telescope	
Primary	f/10, FL = 3910 mm, D = 391 mm
Second	f/10, FL = 2000 mm, D = 200 mm
Third (planned)	f/11, FL = 11000 mm, D = 1000 mm
Data Acquisition System	
Mie and Rayleigh scattering	Licel transient recorders, 16 bit, 20 MHz A/D converters and photon-counters maximum count rate 250 MHz
Multi-anode PMT	Single-photon counting, maximum count rate 100 MHz, 50 ns resolution
ICCD	Digitization 16 bit, 32 MHz, minimum gate width 2 ns
EMCCD	Digitization 16 bit, 17 MHz

energies up to 8 J per pulse at the fundamental wavelength of 1064 nm wavelength. This energy output corresponds to a pulse power of more than 500 GW and an average power of more than 50 W;

- an optical parametric oscillator (Horizon OPO) that is optically pumped by the main laser. The OPO emits laser light from the deep UV (192 nm) to the near infrared (NIR) [2750 nm];

- a customized motorized beam combiner that allows for wavelength selection. It can be switched between seven modes, namely emission of (1) 1064 nm only, (2) 532 nm only, (3) 355 nm only, (4) 1064 and 532 nm (simultaneously), (5) 1064, 532, and 355 nm (simultaneously), as well as (6) optimized OPO pumping and (7) side-port emission of laser light for non-lidar applications;

- a Horiba 1250M imaging spectrometer with four exchangeable gratings, dual entrance ports/slits and two exit ports: one imaging (front) and one high spectral resolution (side) port/slit;

- three imaging detectors that can be used with the spectrometer;

- an intensified charge-coupled device camera (ICCD, Princeton Instruments PI-MAX4 1024i-HBf);

- a 32-channel Licel PMT (photo-multiplier tube);

- an electron multiplying charge-coupled device (EMCCD, ANDOR iXon 3);

- three kinds of single detectors: photomultiplier tubes, InGaAs avalanche photodiodes, and silicon photodiodes.

For this lidar system, we specifically developed an optical sub-system that delivers light signals from a set of signal-receiving telescopes (that will provide signals from approximately 100 m to 100 km height above ground, once the setup of three telescopes is complete) to the entrance slit of the main spectrometer. The optical sub-system is based on a commercially available doublet and triplet achromatic lens.

The design of the optical sub-system was developed based on ZEMAX simulations and experimental tests that were carried out subsequently. The optical components allow for focusing the backscattered light that comes from the receiver telescopes on the entrance slit of the spectrometer with a minimum focal point size. In this way, we are able to obtain an optimal ratio between spectral resolution and intensity of the Raman signals within the spectral range from UV (300 nm) to NIR (1500 nm).

The system allows for using three types of data acquisition modes. We can detect lidar signals on the basis of (a) the use of single detectors, (b) the simultaneous detection of multi-channel spectroscopically resolved lidar signals, and (c) swapping the range of the wavelengths for the imaging detectors.

Depending on the setup of the experiment, the lidar instrument can be used as a (a) multiwavelength elastic backscatter lidar for the measurements of aerosols and temperature from the troposphere to the mesosphere, (b) multi-channel spectroscopic Raman lidar (using Stokes and anti-Stokes, rotational, and rotational-vibrational Raman scattering), (c) multi-channel spectroscopic photoluminescence/fluorescence lidar, (d) high spectral resolution lidar (HSRL), (e) polarization lidar, (f) infrared absorption lidar by scanning the wavelengths generated by an OPO, and (g) differential absorption lidar based on simultaneous emissions from the OPO and one of three main wavelengths of the laser (355, 532, or 1064 nm).

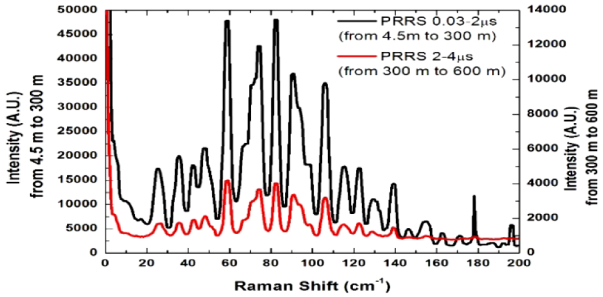

Fig. 1. PRR spectrum of air. Data were acquired at 2017 UTC on 4 November 2017. The signals were averaged over 10 shots (1 s). Laser pulse energy, 300 mJ at 354.9 nm. ICCD time gate: black curve, 0.03–2.00 μs (4.5–300.0 m); red curve, 2–4 μs (300–600 m). Grating, 1200 g/mm. Entrance slit, 50 μm. Resolution, ≈5 cm^{-1}.

Figure 1 shows the results of the Stokes part of PRR scattering measurements with the ICCD camera and the Horiba 1250M spectrometer. The emitted laser pulse energy was 300 mJ at 354.9 nm. The spectrum was averaged over 10 laser shots, and the signal background has been subtracted. The spectrum was taken using the full vertical binning (FVB) mode of the ICCD camera. In this mode, the photons are summarized over those vertical columns of the ICCD pixels that significantly increase the signal-to-noise ratio if spectra are horizontally distributed. The time gate of the camera was set from 0.03–2.00 μs (4.5–300.0 m, black curve) to 2–4 μs (300–600 m, red curve) with respect to the time the laser shots were fired. The spectrometer grating was set to 1200 g/mm. In combination with the 50 μm entrance slit, we obtain a spectral resolution of less than 5 cm^{-1}. This number was calculated on the basis of the Czerny–Turner spectrometer equation using the number of the spectrometer's focal length, the grating size and dispersion, the size of the entrance slit, and the exit slit (size of the pixels of the detector). According to the full width at half-maximum (FWHM) spectral-resolution criteria the actual resolution is 3.5 cm^{-1}. This resolution can be seen for the line with maximum at 59 cm^{-1} and the line with maximum at 122.5 cm^{-1}. The resolution of 3.5 cm^{-1} corresponds to 0.04 nm when using the wavelength of the pumping laser. A 355 nm RazorEdge ultrasteep long-pass edge filter (Semrock LP02-355RE-25) was used to suppress elastic scattering (at 354.9 nm) of laser light. To allow for the measurements of the spectra below 20 cm^{-1}, the RazorEdge filter was slightly tilted around the axis perpendicular to the incident 0 deg angle axis. This tilt of the filter shifts the cutoff wavelength of the filter to shorter wavelengths. As a result, the rejection of the elastic scattering is slightly reduced. However, the tilting allows for the detection of the PRR scattering with one and the same (maximum) transmission of the edge filter in the range from 5 cm^{-1} to more than 4000 cm^{-1} (see Fig. 1; maximum shown range is 200 cm^{-1}).

The spectra in Fig. 1 clearly show scattering from main air compounds – molecular oxygen (O_2) and nitrogen (N_2). The results are in good agreement with model calculations and experimental results obtained under laboratory conditions (presented on page 282 in [12]) in the spectral range from 20 to 200 cm^{-1}. The PRRS have local maximums in the range from 5 to 20 cm^{-1} and can be related to CO_2 Raman scattering. The PRR spectrum of CO_2 is spread from 5 to 50 cm^{-1}. The maximum intensity of the spectrum is located at approximately 15 cm^{-1} at ambient atmospheric pressure and temperature [13].

The results presented in Fig. 1 demonstrate some significant advantages of this spectroscopic approach over the traditional method of using two-channel (or multi-channel) lidars for detecting PRRS of air molecules: (1) LiSsI allows for the direct, range-resolved measurements of entire PRRS of (trace) gases with high spectral resolution; (2) spectra can be taken simultaneously at 1024 channels without the need for scanning across the required wavelength range; (3) the system is designed in a way that allows for observations of PRRS for any excitation wavelength from 300 to 700 nm. With this design, we can easily change to another pumping wavelength without changing significant parts of the experimental setup, which would become necessary in the case of using an interference filter or Fabry–Perot etalons, for example.

Figure 2 shows an example of rotational-vibrational Raman spectra (RVRS). Shown are the experimentally measured distributions of the (1-0) rotation-vibration Raman band of nitrogen molecules as a function of the wavenumber corresponding to the Stokes shift. The spectra represent the altitude range from 150 m to 10 km. The vertical resolution is 15 m. Figure 2 shows three typical spectra taken at 1200, 2700, and 4005 m above ground. The emitted laser pulse energy was 1100 mJ at 354.9 nm. The lidar signals/spectra were obtained by the 32-channel lidar detector (Licel SP32-20). The measurements were carried out at nighttime on October 19, 2018, after sunset (18:50 UTC). The signal-integration time was 209 min (125576 laser shots). The system conditions are described in the figure caption.

The center of the Q branch of the (1-0) band was observed at approximately 2330 cm^{-1} in all altitude levels. Figure 2 clearly shows the O- (2175−2300 cm^{-1}) and S- (2355−2555 cm^{-1}) rotational-vibrational branches, separately from the Q branch.

The obtained spectra are in good agreement with RVRS measured under laboratory conditions by Barrett and Adams [14], as well as numerical calculations [15]. The relative ratios of the O and S branches to the Q branch are also in good agreement with theoretically calculated values.

The spectral resolution achieved under experimental conditions in the case of Fig. 2 (1200 g/mm grating, 50 μm entrance slit, and Licel SP32-20 detector with 0.8 mm) is insufficient to separate the individual rotational-vibrational lines. However, the resolution and signal intensity of the RVRS of nitrogen are sufficiently high for measurements of

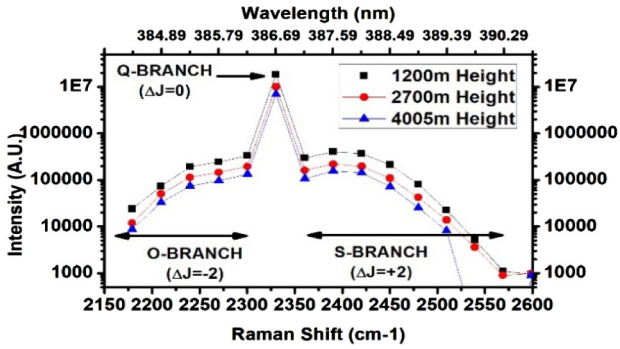

Fig. 2. RVRS of air nitrogen molecules. The signals were acquired between 2030 and 2359 UTC on 19 October 2018 and averaged over 125576 shots (209 min). Laser pulse energy, 1100 mJ at 354.9 nm. Grating, 1200 g/mm. Entrance slit, 50 μm, corresponding to a spectral of resolution ≈ 25 cm^{-1}, i.e., 0.45 nm.

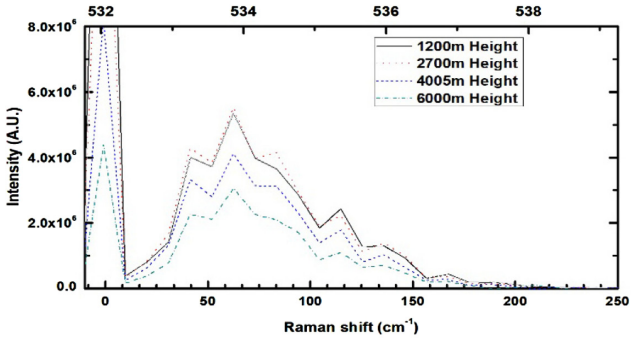

Fig. 3. PRRS of air. The corresponding signals were averaged over 142,347 laser shots (about 4 h) for four selected height levels.

atmospheric temperature profiles up to several kilometres above ground. The Q branch of the Stokes nitrogen component (2330 cm^{-1}) is widely used for aerosol extinction and backscatter profiling. The results presented in Fig. 2 show the potential of using high-resolution spectroscopic lidars. This type of lidar allows for the simultaneous, vertically resolved profiling of temperature, aerosol extinction, and backscattering.

The technical specifications of this spectroscopy lidar result in a significantly increased signal-to-noise ratio and thus allow for carrying out daytime Raman signal observations at VIS and the near UV spectral range. We can use two methods. One is the use of ultra-high pumping energy. The energy of these pulse energies is approximately 10 to 100 times higher than the pulse energy of commonly used Raman lidar systems. The second method is the use of a considerably better bandwidth of the signal receiver system than what is typically used. The receiver system of the spectrometric lidar system has a spectral resolution of better than 1 cm^{-1} (0.036 at 607 nm). That resolution is approximately 10 to 50 times better than the typical spectral resolution of conventional nitrogen Raman lidars which use an interference filter with 0.5 to 2 nm FWHM, which translates to 13 to 55 cm^{-1} at 607 nm. Both approaches allow us to increase the signal-to-noise ratio to a level that allows for measuring vibrational-rotational Raman lidar signals at daytime conditions up to tropopause heights.

Figure 3 shows the results of daytime PRR experiments carried out between 1647 UTC and 2045 UTC on June 11, 2018. Sunset on that day was at 2017 UTC. The profiles were vertically smoothed with a window length of 150 m.

The laser pulse energy was set to 2200 mJ at 532.08 nm. The laser was operated in seeded mode. We used the 32-channel PMT. The size of a single detector element is 0.8 mm. The spacing of the individual anodes is 1 mm. The grating was 2400 g/mm. The entrance slit was set to 50 μm. The spectral resolution was approximately 0.325 nm, obtained experimentally by measurements of the spectral difference between the 576.96 and 579.07 nm lines of a mercury pencil lamp. Figure 3 shows daytime PRRS at 1200, 2700, 4005, and 6000 m height above ground.

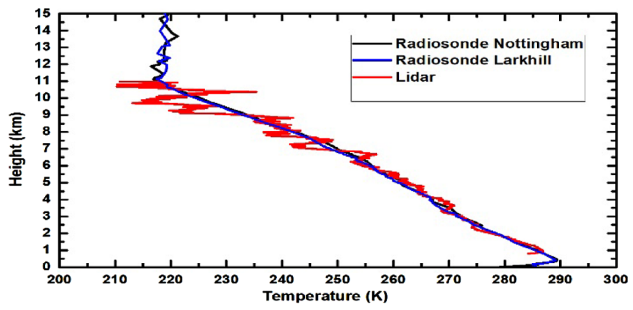

Fig. 4. Temperature profile obtained from PRR lidar signals taken between 1647 UTC and 2045 UTC on 11 June 2018.

Figure 4 presents the daytime profile of atmospheric temperature for the altitude range from 1 to 10 km. The values were obtained using the methods developed by Arshinov *et al.* [9]. The temperature profile is obtained by high-J transmission at 41 cm^{-1} (533.26 nm) and low-J transmission at 115 cm^{-1} (535.36 nm). For comparison, we show the two temperature profiles obtained with radiosondes launched at Nottingham, about 200 km north (black curve) of Hatfield and at Larkhill, about 200 km west (blue curve) of Hatfield. The results show good agreement to the data acquired with both radiosondes in the height range from 1 to 15 km. The difference is less than ±2 K in the height range from 1−6-km and ±10 K from 6 to 11 km height above ground for both meteorological stations.

Funding. University of Hertfordshire; Royal Society (WM120052); Research Executive Agency (708227).

Acknowledgment. This work was supported by the University of Hertfordshire through capital investment. Boyan Tatarov was supported by a Marie-Skłodowska-Curie Action Fellowship of the European Commission (CAPABLE, H2020-MSCA-IF-2015), Grant No: 708227. Detlef Müller was supported by the Royal Society. The authors are grateful for the support work provided by Dr. Matthias Tesche and Dr. Sung-Kyun Shin, formerly at the University of Hertfordshire. Dr. Tesche now is with the University of Lepizig, Germany. Dr. Shin is with the Seoul Institute of Technology, Republic of Korea.

Disclosures. The authors declare no conflicts of interest.

Data Availability. Data underlying the results presented in this paper are not publicly available at this time but may be obtained from the authors upon reasonable request.

REFERENCES

1. M. C. Weitkamp, ed., *LIDAR : Range-Resolved Optical Remote Sensing of the Atmosphere*, Vol. **102** of Springer Series in Optical Sciences (Springer, 2005).
2. R. M. Measures, *Laser Remote Sensing* (Wiley, 1984).
3. A. Ansmann, M. Riebesell, and C. Weitkamp, Opt. Lett. **15**, 746 (1990).
4. P. Piironen and E. W. Eloranta, Opt. Lett. **19**, 234 (1994).
5. D. Müller, U. Wandinger, and A. Ansmann, Appl. Opt. **38**, 2346 (1999).
6. D. Müller, E. Chemyakin, A. Kolgotin, R. A. Ferrare, C. A. Hostetler, and A. Romanov, Appl. Opt. **58**, 4981 (2019).
7. D. Müller, C. A. Hostetler, R. A. Ferrare, S. P. Burton, E. Chemyakin, A. Kolgotin, J. W. Hair, A. L. Cook, D. B. Harper, R. R. Rogers, R. W. Hare, C. S. Cleckner, M. D. Obland, J. Tomlinson, L. K. Berg, and B. Schmid, Atmos. Meas. Tech. **7**, 3487 (2014).
8. A. Cohen, J. A. Cooney, and K. N. Geller, Appl. Opt. **15**, 2896 (1976).
9. Yu. F. Arshinov, S. M. Bobrovnikov, V. E. Zuev, and V. M. Mitev, Appl. Opt. **22**, 2984 (1983).
10. Y. Arshinov, S. Bobrovnikov, I. Serikov, A. Ansmann, U. Wandinger, D. Althausen, I. Mattis, and D. Müller, Appl. Opt. **44**, 3593 (2005).
11. I. Veselovskii, D. N. Whiteman, M. Korenskiy, A. Suvorina, and D. Pérez-Ramírez, Atmos. Meas. Tech., **8**, 4111 (2015).
12. B. Schrader, *Infrared and Raman Spectroscopy: Methods and Applications* (Wiley, 1995).
13. J. J. Barrett and A. Weber, J. Opt. Soc. Am. **60**, 70 (1970).
14. J. J. Barrett and N. I. Adams, J. Opt. Soc. Am. **58**, 311 (1968).
15. H. Inaba and T. Kobayasi, Opto-electron. **4**, 101 (1972).